Studies of Nano-sized Co_3O_4 as Anode Materials for Lithium-ion Batteries

HUANG, Feng[a,b] **(黄峰)** **ZHAN, Hui**[a] **(詹晖)** **ZHOU, Yun-Hong**[*,a] **(周运鸿)**

[a] *College of Chemistry and Molecular Science, Wuhan University, Wuhan, Hubei 430072, China*

[b] *College of Chemical Engineering, Resource and Environment, Wuhan University of Science and Technology, Wuhan, Hubei 430081, China*

The structural evolution of the Co_3O_4 fine powders prepared by rheological phase reaction and pyrolysis method upon different temperature has been investigated using X-ray diffraction (XRD) topography. The electrochemical performance of Co_3O_4 electrode materials for Li-ion batteries is studied in the form of Li/Co_3O_4 cells. The reversible capacity as high as 930 mAh/g for the Co_3O_4 sample heat-treated at 600 ℃ is achieved and sustained over 30 times charge-discharge cycles at room temperature. The detailed information concerning the reaction mechanism of Co_3O_4 active material together with lithium ion is obtained through *ex-situ* XRD topography, X-ray photoelectron spectroscopy (XPS) analysis and cyclic voltammetry (CV) technique. And it is revealed that a "two-step" reaction is involved in the charge and discharge of the Li/Co_3O_4 cells, in which Co_3O_4 active material is reversibly reduced into $xCo\cdot(3-x)CoO$ and then into metallic Co.

Keywords cobalt oxide, anode material, lithium ion battery, rheological phase reaction

Introduction

The large capacity and high cell voltage of lithium-based cells, coupled with their relatively low environmental impact make them an ideal candidate for portable power supplies. Study on present materials for lithium ion batteries focuses on improving cycle ability and increasing capacity of electrode materials.

As one of the important parts of lithium-ion batteries, anode materials have been investigated intensively. Now, carbonaceous materials are used in nearly all lithium ion batteries because of their high capacity (theoretical capacity of 372 mAh/g based on LiC_6). Although commercial carbonaceous materials have exhibited reasonable behavior, there are certain limitations. Upon the intercalation of one lithium ion per six carbons, the lattice parameter of carbonaceous materials increases substantially and causes swelling of the anode and eventual capacity loss of anode material. In addition, the irreversible capacity loss caused by solvent co-intercalation in the first charge-discharge requires more cathode material to balance the cell.

In recent years, some possible alternative systems, such as tin oxide-based electrodes,[1-5] composite negative alloy electrodes[6,7] and lithiated vanadium oxide-based electrodes[8] have received a great deal of attention. However, the poor capacity retention of these materials during cycling, and more especially, large irreversible capacity observed during the first charge-discharge cycle of these materials[9], have limited their use in practical cells. The cobalt oxides (CoO and Co_3O_4) as anode materials for lithium ion batteries were reported by Poizot.[9,10] According to Poizot, these materials provide a very high reversible capacity of 700—1000 mAh/g, which is about two fold the theoretical capacity of carbon and shows good cycle ability.

Co_3O_4 has considerable potential for use in metal-air batteries and fuel cells because it can catalyze molecular oxygen reduction to O^{2-} ion in alkaline solution.[11,12] A variety of methods, such as chemical spray pyrolysis,[13] liquid-control precipitation,[14] sol-gel method,[11] *etc.*, have been used to prepare Co_3O_4 powders and films. In this paper, rheological phase reaction[15] and pyrolysis method were used to prepare nano-sized Co_3O_4 powders. The structural evolution upon heat-treatment temperature was characterized by XRD spectrum. Electrochemical tests were performed to examine Co_3O_4 properties as an anode material for lithium ion batteries. The reaction mechanism of the Co_3O_4 with lithium ion in charge and discharge process was studied by *ex-situ* XRD, XPS and CV curve.

Experimental

Material preparation and characterization

The cobalt hydroxide [$Co(OH)_2$] and oxalic acid ($H_2C_2O_4\cdot 2H_2O$) (analytical reagent grade) were fully mixed by grinding in 1∶1 molar ratio, a proper amount of water was added to obtain the solid-liquid rheologoical state (semisolid state) mixture. The mixture was reacted at

* E-mail: yhzhou@whu.edu.cn

Received March 24, 2003; revised May 14, 2003; accepted June 18, 2003.

Project supported by the National Natural Science Foundation of China (No. 29833090).

80—90 ℃ for 4 h, and then dried at 100 ℃ to obtain the cobalt oxalate ($CoC_2O_4 \cdot 2H_2O$) precursor. Subsequently, the precursor was pyrolyzed at different temperatures for 3 h in air, then the final product, black-colored powders, was obtained. The XRD was conducted on a Shimadzu XRD-6000 diffractometer (Cu Kα radiation) to reveal the structural evolution of Co_3O_4 upon heat-treatment.

Electrode preparation and electrochemical measurement

The electrochemical cells consisted of a Co_3O_4 working electrode and a lithium foil counter electrode. They were assembled in an Ar-filled glove box with both water and oxygen concentrations less than 5 ppm. The working electrodes were composed of Co_3O_4 powders, carbon black and polytetrafluoro ethylene (PTFE) binder (weight ratio of 85∶10∶5). The electrodes were separated by a cellgard 2400 separator soaked in 1 mol/L solution of $LiClO_4$ dissolved in a 50∶50 volume of ethylene carbonate (EC) and diethyl carbonate (DEC). The cells were discharged and charged between (0.01—3.0) V vs. Li^+/Li at a constant current of 100 mA/g using Arbin BT 2000 testing system. Cyclic voltammogram measurement was carried out on CHI660a electrochemical station using a three-electrode cell, in which lithium metal acted as counter and reference electrodes.

Ex-situ XRD *spectroscopy and* XPS *measurement*

In order to study the reaction mechanism of lithium ion with Co_3O_4 electrode, *ex-situ* XRD and XPS analyses were performed on the Co_3O_4 sample heat-treated at 600 ℃. After discharged to the required capacity, the electrode pellets were removed from the cells and washed twice with dimethyl carbonate (DMC) in the glove box, vacuum dried and then covered with Mylar film to perform XRD and XPS measurement. XPS measurement was conducted employing ESCA-MK photoelectron spectrometer (MgK_2 exciting source).

Results and discussion

Structural evolution of Co_3O_4 *precursor vs. heat-treatment temperature*

Fig. 1 shows the XRD patterns of the Co_3O_4 powders heat-treated at different temperatures. Higher temperature treatment results in stronger and sharper diffraction peaks, indicating better crystallinity. In order to estimate the particle sizes, the Scherrer formula ($D = 0.9\lambda / w \cdot \cos\theta$) was applied to (311) peak, where λ is the X-ray wavelength (0.154 nm), w the X-ray linewidth and θ the diffraction angle. The dependence of the particle sizes upon heat-treatment temperature is shown in Fig. 2a. These values roughly match the average particle sizes estimated from TEM image. The relationship between the logarithm of the particle sizes and the corresponding heat-treatment temperature is given in Fig. 2b. The activation energy of the grain growth is evaluated to be about 0.82 eV from the slopes.

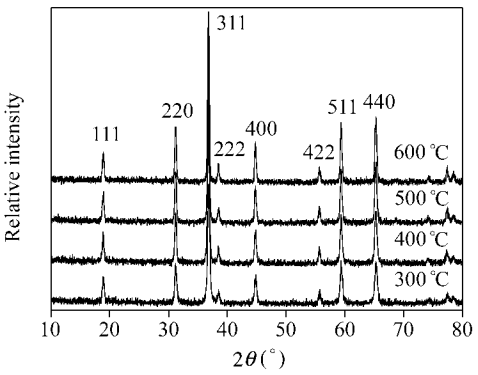

Fig. 1 Evolution of Co_3O_4 XRD peaks upon heat-treatment at different temperatures.

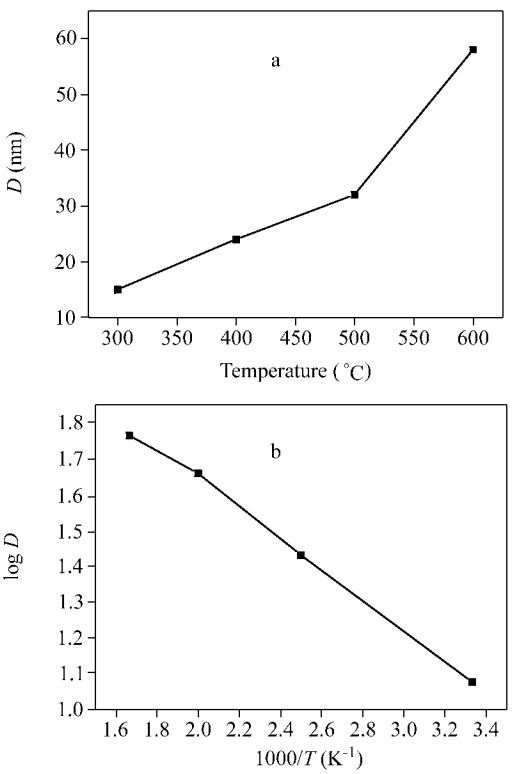

Fig. 2 Variation of the particle sizes as a function of the treatment temperature.

Discharge and charge performances

Fig. 3 shows the initial three discharge and charge curves of Li/nano-sized Co_3O_4 cells with Co_3O_4 heat-treated at 600 ℃. In the first discharge, the potential rapidly drops to a long plateau at about 1.1 V, then drops to a short plateau at about 0.7 V, and then continuously decreases down to 0.01 V, corresponding to one inconspicuous charge slope and one clear charge plateau at about 1.6 V and 2.1 V respectively, indicating a two-step reaction. However, there is only one plateau at 1.25 V in the subse-

quent discharge curves. The similar behaviors are observed for other samples. The subsequent discharge curves differ considerably from the first one, implying drastic, lithium-driven, structural or textural modifications in the first discharge and charge cycle of Co_3O_4 materials,[10] and then accompanied by irreversible capacity. Table 1 shows the first discharge, charge capacity and irreversible capacity loss of Co_3O_4 treated at 600 ℃ vs. different voltage range. It can be seen that the irreversible capacity loss was more sensitive to the upper cutoff potential, while it was essentially unchanged under lower cutoff potentials varying from 0.01 to 0.6 V. The result suggests that irreversible capacity loss is attributed to the reaction occurred at higher potential range. A reversible capacity of more than 900 mAh/g can be obtained for all samples. It is much higher than the theoretical capacity of graphite, 372 mAh/g. Moreover, the Co_3O_4 electrode exhibits a low irreversible loss of about 30% compared to tin-based oxides.[1,4,5]

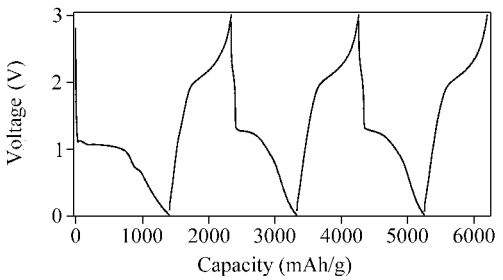

Fig. 3 The initial three cycle curves of the Li/Co_3O_4 cells in which the Co_3O_4 was heat-treated at 600 ℃.

Fig. 4 shows the charge capacity vs. cycle number for Co_3O_4 samples at different heat-treated temperatures. The capacity of each sample slightly increases in initial cycles, indicating that Co_3O_4 electrode material firstly goes through active process during discharge and charge cycling, and the charge/discharge efficiency reaches to 100% after 20 cycles. In addition, the electrochemical properties of Co_3O_4 as anode material for lithium ion batteries are sensitive to its particle sizes, which can be found combining the results indicated in Figs. 2 and 4. The smaller particle sizes are, the higher initial charge capacity and the worse cycle ability will be. Although sample with bigger particle size presents good cycle ability, it shows relatively low initial charge capacity. With increasing of the division degree of nano-particles, the surface Gibbs energy increases gradually. To decrease the surface Gibbs energy of the system, the nanosized particles will aggregate spontaneously, and then result in an undesired cycling performance of electrode material composed of smaller particle size. It is suggested that for the Co_3O_4 materials, an optimum particle size will produce the best state of division of the metal particles, and hence have better electrochemical performance. For the samples heat-treated at 600 ℃, the capacity retention is at its best during cycling over the entire voltage range of 0.01—3.0 V, and can sustain good rate capabilities, being able to deliver 80% of their total capacity at a 2 C rate (see Fig. 4 inset). The results are in agreement with those of Poizot's work.

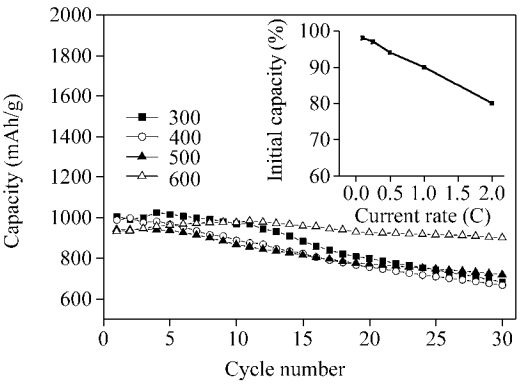

Fig. 4 Cycling performance of the Co_3O_4 treated at different temperatures.

Cyclic voltammetry

The lithium insertion and deinsertion behavior of the Co_3O_4 samples was also investigated using slow scan dynamic voltammogram. Fig. 5 shows the first and the second cycle sweep curves of the Co_3O_4 sample heat-treated at 600 ℃, starting from the open voltage and after that cycled between 0.01 and 3.0 V. In the first sweep cycle, one large dominant reduction peak at about 1.1 V, one small reduction peak at about 0.7 V and corresponding two oxidation peaks at about 1.6 V and 2.1 V are clearly observed respectively. However, the features exhibited on the first sweep curve are not existent on the second and subsequent sweep cycles. The resemblance to the results indicated by discharge and charge test also reveals a "two-step" reaction mechanism.

Table 1 The first discharge, charge capacity and capacity loss of Co_3O_4 electrode heat-treated at 600 ℃ vs. different discharge charge potential scope

Voltage range (V)	First discharge capacity[a] (mAh/g)	First charge capacity (mAh/g)	Irreversible capacity loss (%)
0.01—3.0	1460	986	32.4
0.20—3.0	1307	878	32.8
0.6—3.0	1054	716	32
0.6—2.5	1056	647	38.7

[a] Starting from the open cell voltage.

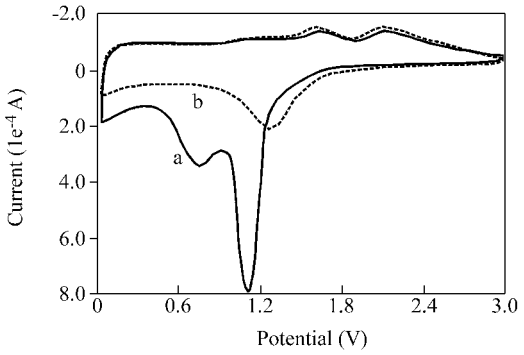

Fig. 5 Cyclic voltammetry curves of the Co_3O_4 electrode heat-treated at 600 ℃. Sweep scope: 0.01—3.0 V vs. Li^+/Li; sweep rate: 0.1 mV/s; electrode area: 0.5 cm^2.

Ex-situ XRD *and* XPS *studies*

Fig. 6 shows the evolution of the XRD patterns (obtained under the same diffraction conditions and recorded with the same scale) of the Co_3O_4 electrode material heat-treated at 600 ℃ on different discharge and charge states. The "fresh" Co_3O_4 sample adopts a spinel structure, and the most intense line is (311), with the value of 2θ being 36.84°. During discharge, the intensities of XRD peaks gradually reduced, and finally vanished when the "Co_3O_4" electrode is discharged to the capacity of 1291 mAh/g, indicating a complete breakdown of Co_3O_4 lattice. The featureless XRD pattern do not evolve upon further reduction down to 0.01 V (corresponding to 1410 mAh/g discharge capacity). Moreover, the characters presented in the XRD pattern of a "fresh" Co_3O_4 electrode cannot be recovered by a recharge operation. No obvious shift in diffraction angle can be observed from Fig. 6, which eliminates the possibility of lithium ion inserting into the Co_3O_4 lattice. The results imply that the Co_3O_4 material could decompose into nano-size metallic Co particle[10] or become amorphous-like structure after being discharged to a certain state, and those nano-particles are smaller than the X-ray coherence length. Therefore, no diffraction peaks are observed.

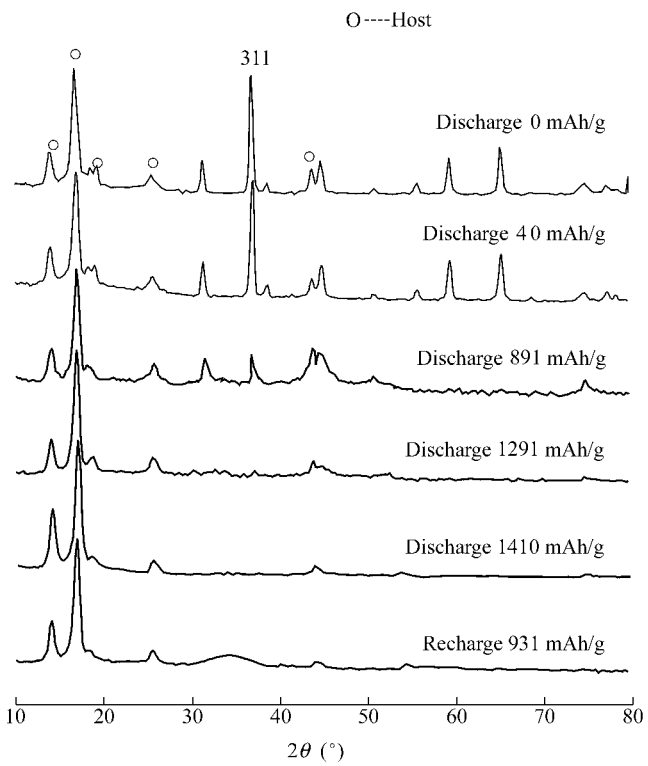

Fig. 6 Evolution of *ex-situ* XRD patterns of the Co_3O_4 electrode in the discharge process.

XPS tests further confirm the results obtained by XRD, as illustrated in Fig. 7. Fig. 7a is the Co_{2p} spectrum of the pristine sample. A main peak at 780.3 eV can be clearly seen, which is attributed to the binding energy in Co_3O_4. The Co_{2p} spectrum of the Co_3O_4 sample, heat-treated at 600 ℃ discharged to 825 mAh/g and 1407 mAh/g, are shown in Fig. 7b and Fig. 7c respectively. The peak at 778.3 eV designated as the binding energy of metallic Co can be observed in both Fig. 7b and Fig. 7c.[16] In addition, a small shoulder peak at about 780.2 eV appears in Fig. 7b. The higher energy component at 780.2 eV is corresponding to the binding energy of CoO.[16] The results indicate that Co_3O_4 is reduced to metallic Co via the mixture of Co and CoO in the discharge process.

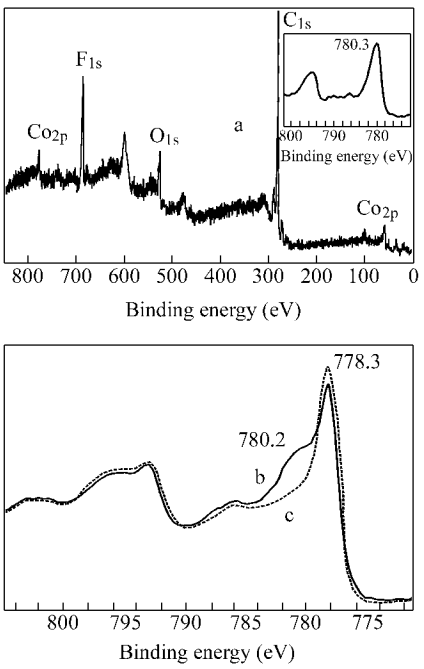

Fig. 7 Evolution of the XPS spectrum of the Co_{2p} in a pristine Co_3O_4 sample upon discharging: (a) pristine sample, (b) discharge 891 mAh/g, (c) discharge 1410 mAh/g.

Mechanism of lithium ion reaction with Co_3O_4 *electrode*

Poizot *et al*.[10] have studied the mechanism of Li-ion insertion into CoO electrode through the *in-situ* XRD spectroscopy analysis of different discharge capacity and indirectly deducing from previous high-resolution electron microscopy (HREM). They suggested that the electrochemical reaction of CoO, which differs from the classical inser-

tion/deinsertion or Li-alloying process, consisted of the reduction of CoO into a composite electrode containing metal nanoparticles dispersed into a Li_2O matrix, followed upon the subsequent charge by the re-oxidation of Co0 to CoO nanoparticles together with the decomposition of Li_2O according to the following equation:

$$CoO + 2Li^+ + 2e^- \Leftrightarrow Co + Li_2O \quad (1)$$

This mechanism can be also spread to other nanosized transitional metal oxides (M_xO_y).[17]

$$M_xO_y + 2yLi^+ + 2ye^- \Leftrightarrow xM^0 + yLi_2O \quad (2)$$

Whereas in our experiments, two processes reaction are derived either from charge and discharge curves or from CV curves. Considering all these facts, a two-step reaction process can be proposed:

$$Co_3O_4 + 2(1+x)Li^+ + 2(1+x)e^- \Leftrightarrow xCo\cdot(3-x)CoO + (1+x)Li_2O \quad (1.5 < x < 3) \quad (3)$$

$$+ \quad xCo\cdot(3-x)CoO + 2(3-x)Li^+ + 2(3-x)e^- \Leftrightarrow 3Co + (3-x)Li_2O \quad (4)$$

$$Co_3O_4 + 8Li^+ + 8e^- \Leftrightarrow 3Co + 4Li_2O \quad (5)$$

Moreover, Co^0 re-oxidized should be responsible for irreversible capacity (as shown in Table 1). This independent result is consistent with the mechanism of Poizot and Larcher proposed based on the *in-situ* X-ray studies and HREM.[10,18]

Conclusions

The rheological phase reaction and pyrolysis method was employed in the preparation of nano-sized Co_3O_4 powders. An optimized electrochemical performance of Co_3O_4 electrode materials can be achieved through controlling the pyrolysis temperature. The cobalt oxides have considerable potential for use in low voltage Li-ion battery. It can show over 630 mAh/g reversible capacity when cycled between (0.6—2.5) V and good cycling performance. Moreover, the higher lithium insertion potential makes cells safer. However, the cobalt oxides also suffer from an irreversible capacity loss during the first cycle, and seeking a solution to the capacity loss is being in progress.

A two-step reaction mechanism of the cobalt oxides with lithium is proposed on the basis of the result of *ex-situ* XRD, XPS and cyclic voltammogram, and it can be described as the following equations:

$$Co_3O_4 + 2(1+x)Li^+ + 2(1+x)e^- \Leftrightarrow xCo\cdot(3-x)CoO + (1+x)Li_2O$$

and

$$xCo\cdot(3-x)CoO + 2(3-x)Li^+ + 2(3-x)e^- \Leftrightarrow 3Co + (3-x)Li_2O.$$

Further experiments are still being proceeded in our laboratory to obtain more information concerning the mechanism of Li-ion insertion into Co_3O_4 anodes.

Acknowledgments

We express our sincere gratitude to Doctor Zhengyong Yuan and Professor Jutang Sun for offering us the preparation method of Co_3O_4 samples.

References

1 Stefan, M.; Takahisa, S.; Yoji, S.; Junichi, Y. *J. Power Source* **1998**, *73*, 216.
2 Lee, J. Y.; Zhang, R. F.; Liu, Z. L. *J. Power Source* **2000**, *90*, 70.
3 Mohamedi, M.; Seo, J.; Takahshi, D.; Nishizawa, I. M. T.; Uchida, I. *Electrochim. Acta* **2001**, *46*, 1161.
4 Belliard, F.; Connor, P. A.; Irvine, J. T. S. *Solid State Ionics* **2000**, *135*, 163.
5 Yuan, Z. Y.; Huang, F.; Sun, J. X.; Zhou, Y. H. *Chem. Lett.* **2002**, *3*, 408.
6 Mao, O.; Dunlap, R. A.; Dahn, J. R. J. *Electrochem. Soc.* **1999**, *146*, 405.
7 Kepler, K. D.; Vaughey, J. T.; Thackeray, M. M. *Electrochem. Solid-State Lett.* **1999**, *2*, 307.
8 Denis, S.; Baudrin, E.; Touboul, M.; Tarascon, J. M. *J. Electrochem. Soc.* **1997**, *144*, 4909.
9 Badway, F.; Plitz, I.; Grugeon, S.; Tarascon, J. M. *Electrochem. Solid-State Lett.* **2002**, *5*, A115.
10 Poizot, P.; Laruelle, S.; Grugeon, S.; Dupont, L.; Tarascon, J. M. *Nature* **2000**, *407*, 496.
11 Morales, U.; Campero, A.; Solorza-Feria, O. *J. New Mater. J. Electrochem. Syst.* **1999**, *2*, 89.
12 Singh, J. P.; Singh, R. N. *J. New Mater. Electrochem. Syst.* **2000**, *3*, 137.
13 Singh, R. N.; Koening, J. F.; Poillerat, G.; Chartier, P. *J. Electrochem. Soc.* **1990**, *137*, 1408.
14 Li, Y.; He, Y.; Li, L. *Chem. J. Chin. Univ.* **1990**, *20*, 519 (in Chinese).
15 Sun, J.; Xie, W.; Yuan, L.; Zhang, K.; Wang, Q. *Mater. Sci. Eng.* **1999**, B*64*, 157.
16 Moulder, J. F.; Stickle, W. F.; Sobol, P. E.; Bomben, K. D. In *Handbook of X-Ray Photoelectron Spectroscopy*, Ed.: Chastain, J., Published by Pekin-Elmer Corporation Physical Electronics Division, 6509 Flying Cloud Drive Eden Prairie, Minnesota 55344 United States of America, **1996**.
17 Dolle, M.; Poizot, P.; Dupont, L.; Tarascon, J. M. *Electrochem. Solid-State Lett.* **2002**, *5*, A18.
18 Larcher, D.; Sudant, G.; Leriche, J. B.; Chabre, Y.; Tarascon, J. M. *Electrochem. Solid-State Lett.* **2002**, *149*, A234.

(E0303246 ZHAO, X. J.; LU, Z. S.)